RESEARCH ARTICLE

Genotoxicity of dietary, environmental and therapeutic topoisomerase II poisons is uniformly correlated to prolongation of enzyme DNA residence

Faiza M. Kalfalah[1], Christian Mielke[1], Morten O. Christensen[1], Simone Baechler[2], Doris Marko[2] and Fritz Boege[1]

[1] Institute of Clinical Chemistry and Laboratory Diagnostics, Heinrich-Heine-University, Medical Faculty, Düsseldorf, Germany
[2] Department of Food Chemistry and Toxicology, University of Vienna, Vienna, Austria

Received: October 12, 2010
Revised: January 15, 2011
Accepted: January 21, 2011

Scope: DNA damage by genistein and etoposide is determined by the half-life of topoisomerase II–DNA linkage induced [Bandele O. J. and Osheroff N., *Biochemistry* 2008, *47*, 11900]. Here, we test whether this applies generally to dietary flavonoids and therapeutic compounds enhancing topoisomerase II–DNA cleavage (Topo II poisons).

Methods and results: We compared the impact of Topo II poisons on DNA residence kinetics of biofluorescent human topoisomerases IIα and IIβ (delineating duration of the DNA-linked enzyme state) with histone 2AX phosphorylation (delineating DNA damage response). Prolongation of topoisomerase II–DNA residence was correlated to DNA damage response, whereas topoisomerase II–DNA linkage was not. Catalytic inhibitors stabilizing topoisomerase II on unbroken DNA also exhibited such a correlation, albeit at a lower level of DNA damage response. Therapeutic Topo II poisons had stronger and more durable effects on enzyme II DNA residence and elicited stronger DNA damage responses than natural or dietary ones.

Conclusions: Topoisomerase II-mediated DNA damage appears related to the prolongation of enzyme DNA residence more than to enzyme–DNA cleavage. Due to this reason, genistein and other tested natural and dietary Topo II poisons have a much lower genotoxic potential than therapeutic ones under the conditions of equal topoisomerase II–DNA linkage.

Keywords:
Anti-cancer drugs / Bio-flavonoids / DNA damage / DNA topoisomerase II / Genotoxicity

1 Introduction

Isoflavones represent the major flavonoids in soy and soy-based products [1–3]. Epidemiological studies indicating a lower risk of breast and prostate cancer in Asian populations with high intake of soy have opened new markets for soy-based products in western countries especially on the exponentially growing field of food supplements [4]. However, targeting of human topoisomerases is discussed as a potentially adverse effect of this class of compounds, which might be of relevance for the maintenance of DNA integrity [5]. A variety of compounds stimulate DNA double-strand breakage through interference with the cleavage/ligation reaction of DNA topoisomerase II (Topo II). Such agents are termed Topo II poisons. They are chemically diverse encompassing some of the most powerful anticancer drugs [6], a range of widely consumed plant polyphenols [7], various plant alkaloids and fungal toxins [8–10], and certain benzoquinone metabolites of therapeutics or industrial chemicals [11–13]. Common to these compounds is the enhancement of Topo II–DNA cleavage in vitro and in vivo. However, the genotoxic and cytotoxic potency ensuing

Correspondence: Professor Fritz Boege, Institute of Clinical Chemistry and Laboratory Diagnostics, Heinrich-Heine-University, Moorenstrasse 5, D-40225 Dusseldorf, Germany.
E-mail: boege@med.uni-duesseldorf.de
Fax: +49-211-8118021

Abbreviations: AOH, alternariol; **DOX,** doxorubicine; **EGCG,** (-)epigallocatechine-3-gallate; **FRAP,** fluorescence recovery after photopbleaching; **GFP,** green fluorescent protein of *Aequorea victoria*; **γH2AX,** histone 2AX phosphorylated at serine 139; **ICRF-187,** dexrazoxane (Zinecard); **mAMSA,** *m*-amsacrine; **MITOX,** mitoxantrone; **NAPQI,** *N*-acetyl-*p*-benzoquinone imine; **Topo II,** DNA topoisomerase II; **VP16,** etoposide; **YFP,** yellow fluorescent variant of GFP

thereof varies by orders of magnitude. For instance, genistein (a plant polyphenol enriched in soy products [1]) is much less DNA damaging than etoposide (VP16, a widely used anti cancer drug [14]) under conditions where the two compounds are roughly equivalent in terms of Topo II DNA cleavage stimulation [7, 15]. This discrepancy between efficacy at the molecular and the cellular level could be due to the fact that DNA breakage stimulated by Topo II poisons is reversible and contributes to permanent DNA damage through a dynamic interplay between the catalytic Topo II DNA intermediate and various DNA metabolic processes [6]. A recent study comparing the amount of single- and double-stranded DNA breaks induced by VP16 with corresponding histone 2AX phosphorylation (γH2AX, histone 2AX phosphorylated at serine 139) and colony survival comes to the conclusion that 99% of primary Topo II-mediated DNA breaks neither trigger γH2AX nor contribute to cytotoxicity [16]. Moreover, γH2AX responses and cytotoxicity induced by genistein and VP16 are not correlated to the level of Topo II-mediated DNA strand breakage induced (which is similar for the two agents) but to the persistence of these lesions after washout of the agents (which is much longer for VP16) [17]. In keeping with this, persistent γH2AX responses to transient VP16 exposure seem due not to the trapped Topo II-DNA intermediates per se, but to a long-termed persistence of a subset of Topo II-dependent DNA defects that cannot be properly repaired or removed [18]. γH2AX is a marker of persistent cellular DNA damage response that correlates well with DNA-strand breakage and cell death triggered by Topo poisons [16, 19] or ionizing radiation [20–22]. It is believed to be a biomarker of genotoxicity as reliable as micronuclei or DNA comet assays [23–26]. Therefore, the above findings can be interpreted to suggest that genotoxicity of Topo II poisons is dependent on the half-life rather than the amount of Topo II–DNA intermediates induced and that these two properties are not covariant. Thus, the half-life of Topo II–DNA intermediates induced in a living cell could be a meaningful parameter for genotoxic risk assessment of dietary Topo II poisons.

We have previously determined the mobility of human Topo II in living cells by the recovery of fluorescence recovery after photobleaching (FRAP) of the green fluorescent protein of *Aequorea victoria* (GFP)-fused enzymes. We observed that both isoforms (α and β) have high FRAP rates, indicating free mobility in the nucleoplasm [27], as is the case for most DNA interacting proteins not playing a structural role in the nuclear chromatin [28]. Exposure to the strong Topo II poison teniposide dramatically decreased FRAP rates reflecting a drop in mobility due to enhanced and/or prolonged attachment to DNA (which is virtually immobile) [27]. Bioinformatic modeling infers that such FRAP rates are directly correlated to exchange rates between free and DNA-bound Topo II and inversely correlated to the mean DNA-residence time of the enzymes [29–31]. Thus, the impact of Topo II poisons on the half-life of the DNA-coupled state of biofluorescent Topo II can be quantified in the living cell by nonlinear regression analysis of FRAP kinetics [30, 31]. Here, we study several archetypical Topo II-targeting agents by this approach, comparing drug impact on DNA interaction kinetics of human Topo IIα and IIβ in the living cell with γH2AX as an established endpoint of ensuing DNA damage and genotoxicity [25, 26]. We thus address the question whether alteration of ex vivo mobility of biofluorescent Topo II could be a universal parameter for the genotoxic potential of dietary and therapeutic Topo II poisons.

2 Materials and methods

2.1 Cell culture and -imaging

Human HT-1080 fibrosarcoma cells and human noncancerous MRC-5 lung cells were obtained from the German Collection of Microorganisms and Cell Cultures (Braunschweig, Germany) and the European Collection of Cell Cultures (Salisbury, UK), respectively, and grown as specified by the supplier. Stable expression of full-length, GFP-tagged Topo IIα or Topo IIβ in HT-1080 cells followed the previously published procedures [27, 32]. Epifluorescent images were acquired using an inverted microscope (Axiovert 100, Carl Zeiss, Germany) equipped with a digital camera (Visitron System GmbH, Germany). For live cell imaging, cells were cultured under the microscope in CO_2-independent medium. Confocal imaging and FRAP analysis followed the previously published procedures [27]. All measurements were performed at 37°C using an LSM 510 inverted confocal laser-scanning microscope equipped with a CO_2-controlled on stage heating chamber and a heated 40/1.4 NA oil-immersion objective (Carl Zeiss). For FRAP measurements, a single optical section was monitored. Images were taken before and at 1 s time intervals after bleaching of a small circular area in the nucleus at 20 mW nominal laser power with 15 iterations. Imaging scans were acquired with the laser power attenuated to 0.1–1% of the bleach intensity. For quantitative analysis, fluorescence intensities of the bleached region, the entire cell nucleus, and the extracellular background were measured at each time point. Data were corrected for extracellular background intensity and for the overall loss in total intensity as a result of the bleach pulse itself and the imaging scans. FRAP curves were generated by calculating the relative intensity (I) of the bleached area = (I bleached spot × I entire cell nucleus at time 0)/(I bleached spot at time 0 × I entire cell nucleus) [28]. Nonlinear regression analysis of FRAP curves was carried out as described in [30, 31] using a commercial computer software (GraphPad PRISM 4.0a, GraphPad Software, USA).

2.2 Immunoblotting

Cells were grown on 6-well plates, treated with drugs for 1 h, harvested, lysed with 2% SDS, separated by SDS-PAGE, and blotted onto PVDF membranes (Immobilon P; Millipore, Schwalbach, Germany). Topo II immunoband depletion was assessed in HT-1080 cells expressing GFP-tagged Topo IIα and IIβ. Blots were probed with either a mouse monoclonal antibody against GFP (clone JL8, Clontech, Heidelberg, Germany), a rabbit polyclonal antibody against Topo IIα (H-231; Santa Cruz, USA), or a rabbit polyclonal antibody raised against a peptide of amino acid residues 1586–1621 of human Topo IIβ [33]. H2AX phosphorylation was assessed in untransfected HT-1080 cells and MRC-5 cells. Blots were probed with mouse monoclonal antibody specific for histone H2AX phosphorylated at Ser139 or polyclonal rabbit antibodies against total histone H2AX (JBW301 and 07-627, respectively, Millipore). Blots were developed with peroxidase-coupled secondary antibodies and chemiluminescence was quantified with a digital camera system (LAS 4000, Fuji, Düsseldorf, Germany). Cumulative H2AX phosphorylation determined by immunoblotting showed a good correlation with DNA-damage foci accumulation in non-S-phase HT-1080 cells determined with 53 binding protein 1 (Supporting Information Fig. 1).

2.3 Topo II DNA-cleavage in vitro

Reaction mixtures contained 100 ng TopoIIα or 200 ng Topo IIβ, 400 ng negatively supercoiled pUC18 plasmid and various concentrations of a given Topo II poison in a total volume of 40 μL of cleavage buffer (10 mM Tris-HCl [pH 7.9], 10 mM $MgCl_2$, 100 mM KCl, and 0.1 mM EDTA). Mixtures were incubated at 37°C for 7 min and enzyme–DNA cleavage complexes were trapped by the addition of 5 μL 5% SDS. Proteinase K (5 μL of 1 mg/mL) was added and the samples were incubated at 50°C for 1 h. The samples were mixed with 10 μL of agarose gel-loading buffer and subjected to electrophoresis in 0.8–1% agarose gels containing 0.5 μg/mL ethidium bromide. DNA bands were visualized and cleavage was monitored by the conversion of supercoiled plasmid DNA to linear molecules.

Topo II-DNA linkage ex vivo was analyzed by the ICE-bioassay [34]. Briefly, 3.0 million HT-1080 cells were allowed to grow for 48 h in Petri dishes (diameter, 15 mm) and afterward incubated with the solvent control (1% v/v DMSO), VP16, or genistein for 1 h under serum-free conditions. Cells were harvested and lysed in 6 mL TE-buffer (10 mM Tris, pH 8.0, 1 mM EDTA, and 1% w/v *N*-laurylsarcosyl sodium salt) and cell lysates (4 mL) were layered onto a CsCl gradient in polyallomer tubes (14 mL – SW40, Beckman Coulter GmbH, Krefeld, Germany). One gradient consisted of four layers (2 mL/layer) of CsCl with a decreasing density from the bottom to the top. Following centrifugation (100 000 × *g* for 24 h at 20°C), gradients were fractionated (300 μL/fraction) from the bottom of the tubes and DNA content was determined in each fraction by the absorbance at 260 nm using a NanoDrop spectrophotometer (PeqLab Biotechnologie GmbH, Erlangen, Germany). Fractions were slot blotted onto a nitrocellulose membrane and Topo IIα and IIβ were detected with specific rabbit polyclonal antibodies and anti-rabbit IgG peroxidase conjugates (all from Santa Cruz Biotechnology, Heidelberg, Germany). Chemiluminescent signal (LumiGLO, Cell Signaling Technology, USA) on the blots was measured with a LAS 4000 and analyzed with the Multi Gauge V3.2 software (Fujifilm, USA). Drug-induced increases in DNA linkage of Topo II were expressed as percentage of untreated control (= photon counts of treated cells/photon counts of control cells × 100).

2.4 Topo II-targeted compounds

Pharmaceutical formulations of VP16 and dexrazoxane (ICRF-187) (Bristol, Germany and Zinecard Pharmacia & Upjohn, USA, respectively) were obtained from the local pharmacy. Naphthoquinone, menadione, plumbagine, lawsone, and juglone were kindly supplied by Lars O. Klotz, (Institute of Environmental and Preventive Medicine, IUF, Düsseldorf, Germany). Alternariol (AOH) was prepared as stated in [9]. *m*-Amsacrine (mAMSA), doxorubicine (DOX), mitoxantrone (MITOX), (−)epigallocatechine-3-gallate (EGCG), (−)epicatechin, genistein, quercetin, and *N*-acetyl-*p*-benzoquinone imine (NAPQI) were purchased from Sigma-Aldrich, Germany. Solid substances were dissolved in DMSO and stored at −20°C, except for NAPQI and ICRF-187 which were freshly dissolved in water each time. For treatment with natural polyphenols, the aglycon forms were used and catalase (100 U/mL) was added to the incubation mixtures to prevent oxidative inactivation of the compounds [35].

3 Results

3.1 Characterization of biofluorescent reporter cells based on the HT-1080 cell line

For a precise correlation between drug impact on ex vivo mobility of Topo II and corresponding DNA damage, we constructed biofluorescent reporter cells based on the human fibrosarcoma cell line HT-1080, which has a stable genome and a low background of constitutive DNA damage response (Fig. 1C). Cell clones were established that stably express GFP-fused Topo IIα or IIβ and are similar to the parental cell line both in gross morphology and in cell-cycle duration. Cellular localization and morphology of the two biofluorescent Topo II species (Fig. 1A) conformed to observations made in other human

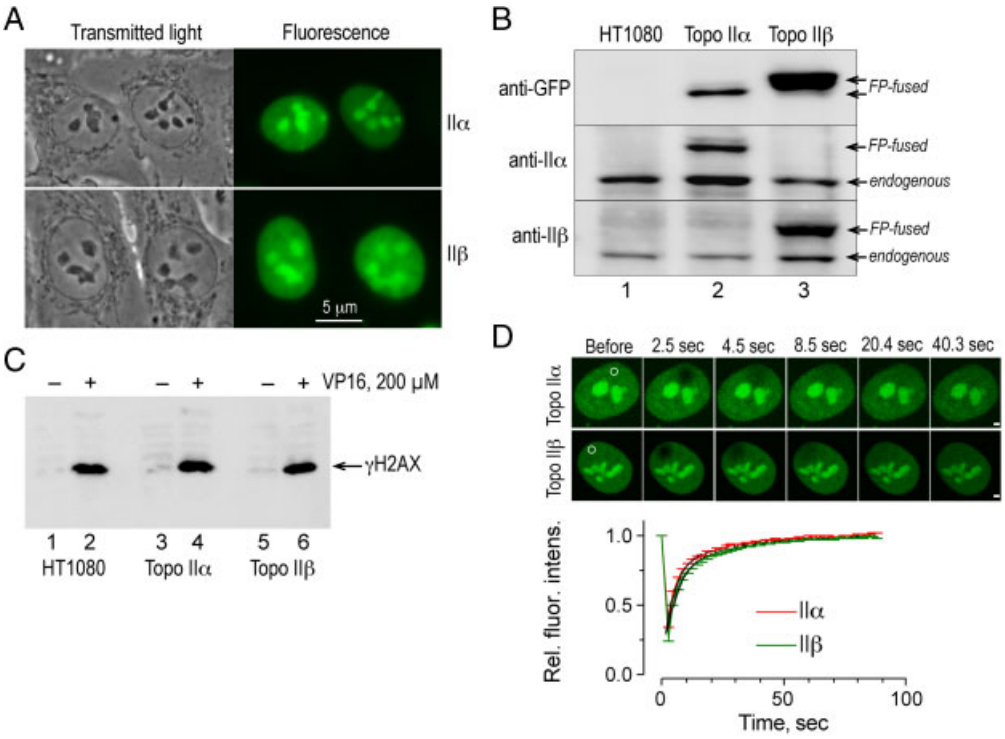

Figure 1. Expression of biofluorescent human Topo II isozymes in human cells. (A) Representative images of HT-1080-cell clones expressing human Topo IIα-GFP (top) or IIβ-GFP (bottom) imaged at 630-fold magnification by transmitted light (left) or green epifluorescence (right). (B) Western blots of whole cell lysates of parental HT-1080 cells (lane 1) and HT-1080 cell clones expressing human Topo IIα-GFP (lane 2) or IIβ-GFP (lane 3) probed with GFP-antibodies (top) or isoform-selective antibodies against C-terminal epitopes of human Topo IIα (middle) and IIβ (bottom), respectively. (C) Parental HT-1080 cells (lanes 1 and 2) and HT-1080 cell clones expressing human Topo IIα-GFP (lanes 3 and 4) or IIβ-GFP (lanes 5 and 6) were cultured for 1 h with (lanes 2, 4, and 6) or without (lanes 1, 3, and 5) 200 μM VP16 for 1 h and then subjected to immunoblotting with a monoclonal γ-H2AX antibody (Ser 139). (D) Representative example of FRAP measurements: Images of HT-1080 cell clones expressing human Topo IIα-GFP (top row) or -IIβ-GFP (bottom row) were taken before and at the indicated times after GFP was bleached in the nucleoplasmic area indicated by a white circle. Relative recovery of fluorescence intensities in the bleached region was continuously recorded over time. The plot at the bottom summarizes the mean (±SEM) of eight independent FRAP recordings made in individual cells and normalized to a prebleach fluorescence level of 1. Error bars indicate the standard error of the mean at selected time points. Black lines represent the results of nonlinear regression analysis of the data using kinetic models assuming the coexistence of two enzyme fractions with different mobilities.

cells by immunohistochemistry [36] or expression of GFP-tagged human enzymes [27, 32]. In Western blots (Fig. 1B, top), GFP-fused Topo IIα or IIβ (lanes 2 and 3, respectively) were detected with GFP antibodies as single protein bands of the expected size (arrows), which were absent in untransfected HT-1080 cells (lane 1). Thus, all GFP fluorescence in the cells could be assigned to GFP fusions of full-length Topo IIα and IIβ. In Western blots probed with isoform-specific antibodies against Topo IIα (Fig. 1B, middle) or IIβ (Fig. 1B, bottom), GFP chimera could be clearly discriminated from corresponding endogenous enzymes because of their slower migrating bands (arrows). Intensity of endogenous and GFP-fused enzyme bands was in a similar range, suggesting that the tracer proteins were not overexpressed and did not significantly increase overall cellular Topo II levels. In keeping with this, the DNA damage response to VP16 (200 μM, 1 h) of the cell clones expressing Topo IIα-GFP or Topo IIβ-GFP was quantitatively similar in terms of H2AX phosphorylation to the parental cell line (Fig. 1C). All three cell lines were virtually negative for H2AX phosphorylation in the absence of VP16, indicating that residual cellular DNA damage levels were also not altered by the expression of GFP-fused Topo II. As will be shown later (Fig. 2C), H2AX phosphorylation (γH2AX) in response to VP16 in these cells was also virtually the same as in noncancerous MRC-5 lung cells.

Mobility of Topo II was characterized by FRAP. FRAP kinetics of biofluorescent, human Topo IIα, or IIβ shown in Fig. 1D were similar to those previously observed in a HEK-293 cell line stably expressing Topo IIβ-GFP or Topo IIα-GFP [27]. Nonlinear regression analysis of FRAP curves was carried out as described previously [30, 31]. Kinetic models assuming the coexistence of one, two, or three individual enzyme fractions with different mobilities were tested and significantly best fits (according to R^2-values of >0.9 and

F-test significances of <0.001) were obtained with the assumption of two individual enzyme fractions (Fig. 1D, bottom, curve fits are superimposed as dotted lines on FRAP recordings). The major component was a rapidly moving fraction with a recovery rate constant $K_{fast} = 0.247 \pm 0.04$ and 0.205 ± 0.01/s for Topo IIα and IIβ, respectively. According to maximal recovery values calculated for the individual components of the curve, the fast fraction made up roughly three quarters of the observed enzyme molecules (78 ± 2 and 76 ± 3% of Topo IIα and IIβ, respectively), whereas the remaining quarter had a ten-fold slower mobility ($K_{slow} = 0.032 \pm 0.009$ and 0.031 ± 0.005/s for Topo IIα and IIβ, respectively). In untreated cells, the observed FRAP curves always converged to a relative fluorescence intensity of 1.0 and values of maximal recovery of fast and slow component derived from nonlinear regression of the curves added up to 100%. Thus, fast and slow enzyme fractions together always accounted for complete recovery of fluorescence in the bleached spot excluding contribution of further, less mobile enzyme subfractions to the observed data. A quantitatively similar distribution of fast and slow fractions has been previously observed for nuclear Topo I [31] and a variety of other nuclear proteins transiently interacting with DNA [28, 30, 37]. Current belief holds that the slow fraction represents protein molecules engaged in DNA association/dissociation processes, whereas the fast fraction represents protein molecules currently not engaged in DNA metabolic processes and therefore more free to roam the nuclear space [27, 28, 30, 37]. Further support of this assumption is lend by the data shown in Fig. 5A and B. In summary, these analyses confirmed that (i) the established cell clones expressed physiological levels of GFP-tagged Topo IIα or IIβ, (ii) the biofluorescent tracer proteins were correctly localized and normally mobile, (iii) the cells expressing the labeled enzymes exhibited an unaltered DNA damage response to a standard Topo II poison, and (iv) the cells had a normal morphology and an undisturbed cell-cycle progression. Therefore, the biofluorescent reporter cells based on the HT-1080 cell line were an adequate model for comparing the impact of Topo II targeted drugs on the ex vivo mobility of Topo IIα and IIβ with cellular DNA damage responses to the drugs judged by H2AX phosphorylation [25].

3.2 VP16 and genistein have a similar impact on Topo II-mediated DNA cleavage in vitro and Topo II–DNA linkage ex vivo but a different impact on H2AX phosphorylation and subnuclear Topo II distribution

Next, we compared the effects of the synthetic podophyllotoxin derivative VP16, a prototypic non-DNA intercalative Topo II poison widely used in cancer therapy [38] and the plant polyphenol genistein, a major component in eastern diets rich in soy [1]. In MRC-5 cells, these two compounds have a similar potency to stimulate Topo II DNA cleavage, but a divergent genotoxic potential [7]. In our cell model, we observed a similar divergence: VP16 and genistein had similar dose–response characteristics with respect to stimulation of Topo II DNA cleavage in vitro (Fig. 2A) and stabilization of the Topo II–DNA intermediate in HT-1080 cells (Fig. 2B), suggesting that the maximal capacity of the two compounds to poison Topo II is similar. However, corresponding measurements of H2AX phosphorylation carried out in HT-1080 and MRC-5 cells (Fig. 2C) revealed that genistein elicited an at least 30-fold lesser DNA damage response than VP16 across a wide concentration range. Interestingly, DNA damage responses to both drugs were correlated to the amount of DNA-linked Topo IIα or IIβ with the result that the regression lines had a ten-fold difference in slope (0.28 versus 0.029 and 0.29 versus 0.03 for Topo IIα and IIβ, respectively; Fig. 2D). This suggests that DNA damage responses to genistein and VP16 are not only governed by the extent of Topo II–DNA entrapment but by at least one more factor. Another notable difference in the cellular response to the two drugs is shown in Fig. 2E: VP16 induced a rapid redistribution of GFP-fused Topo IIα and IIβ from nucleoli to nucleoplasm, which has been previously attributed to fixation of the enzymes at nucleoplasmic DNA sites [27, 31]. On the contrary, genistein at concentrations inducing similar levels of DNA cleavage in vitro or Topo II–DNA entrapment in the cell failed to induce nuclear redistribution of Topo IIα. This further indicates that stimulation of Topo II DNA cleavage and linkage per se does not necessarily disturb the cellular disposition of Topo IIα and IIβ. Thus, the genotoxic action of Topo II poisons must be determined by an additional feature, and the recent studies [17] suggest that this could be prolongation of Topo II–DNA residence time.

3.3 VP16 induces a ten-fold increase in DNA residence times of Topo IIα and IIβ, whereas genistein promotes DNA engagement of Topo II without prolonging DNA residence

To measure Topo II–DNA residence kinetics, we used photobleaching techniques. Upon exposure to increasing VP16 concentrations, Topo IIα and IIβ became progressively less mobile in the cell nucleus, as deducible from a significant retardation of FRAP (Fig. 3A). The mean of 20 individual FRAP recordings covering a time frame from 20 to 40 min after addition of VP16 exhibited a scatter similar to the inherent imprecision of the data (Fig. 1D), indicating that VP16 effects were in the equilibrium after 20 min of exposure. This given, nonlinear regression analysis of serial FRAP curves (Fig. 3A, curve fits are superimposed on FRAP recordings as dotted lines) could be interpreted in quantitative terms quoad equilibrium effects of VP16 on the ex vivo mobility of Topo IIα and IIβ. Up to 50 μM, VP16 best curve fits (according to R^2-values of >0.9 and *F*-test significances of

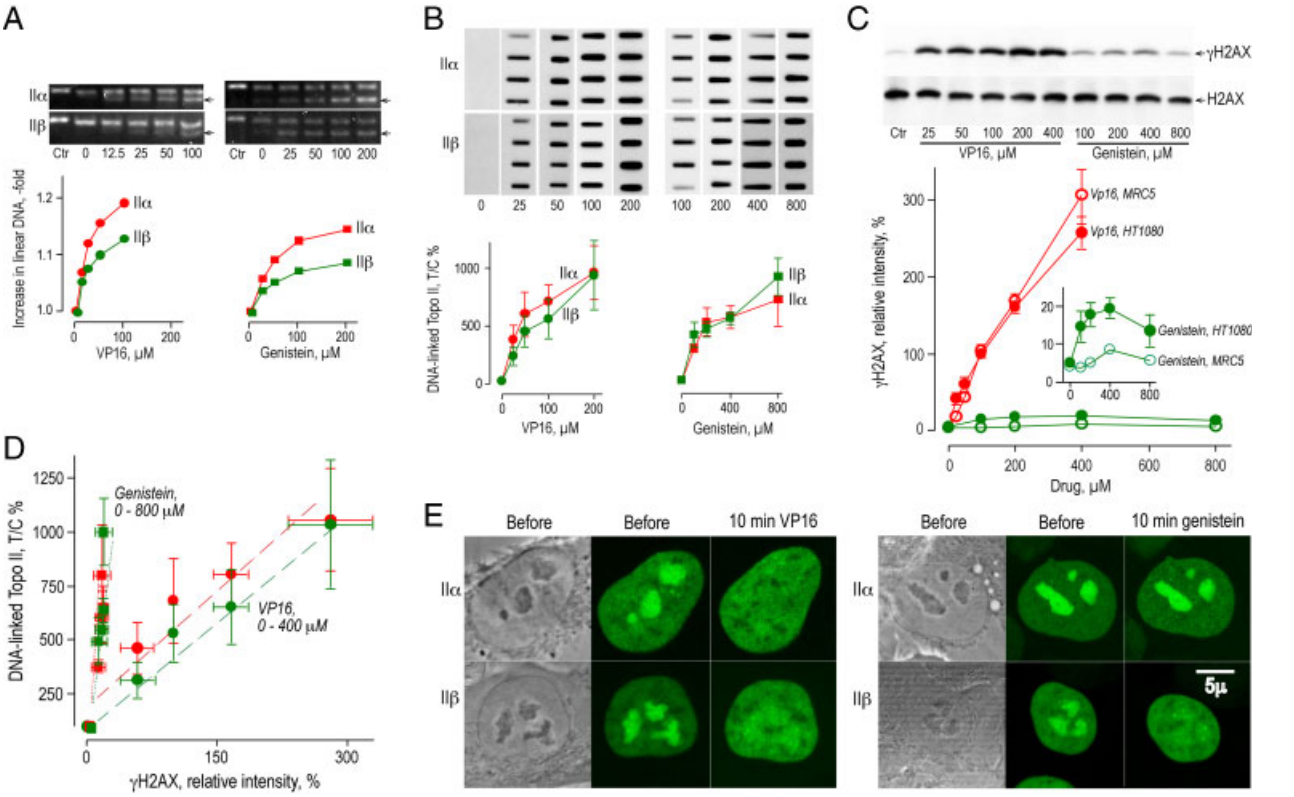

Figure 2. Effects of VP16 and genistein on Topo II-mediated DNA cleavage, trapping of Topo II on DNA, H2AX-phosphorylation, and enzyme localization. Quantitative data referring to Topo IIα and IIβ are indicated by red and green symbols, respectively, whereas data points referring to the effects of VP16 and genistein are shown by circles and squares, respectively. (A) DNA cleavage in vitro: pUC18 plasmid DNA was incubated (20 min, 30°C) with purified human Topo IIα or IIβ and VP16 (left) or genistein (right) at the indicated concentrations. Representative gels are shown on top and intensities of linearized DNA as compared with solvent control are plotted against drug concentration at the bottom. Arrowheads point at linearized plasmid induced by Topo II-mediated DNA cleavage. (B) Topo II–DNA linkage measured by the ICE-bioassay in HT-1080 cells treated with VP16 (left) or genistein (right) at the indicated concentrations for 1 h. Top: Representative results of enzyme–DNA complexes isolated by CsCl-gradient centrifugation and visualized by slot blotting. Bottom: Mean values ± SEM of three similar experiments normalized to cells exposed to the solvent control (set to 100%). (C) Assessment of H2AX phosphorylation by comparative immunoblotting following drug treatment for 1 h. Top, upper blot: Representative result obtained with a monoclonal antibody against γ-H2AX (phosphorylated at Ser 139). Top, lower blot: Corresponding result with a polyclonal antibody against total H2AX. Bottom: Mean ± SEM ($n = 4$) of intensities of γ-H2AX-specific bands plotted against drug concentration. Data were corrected for loading (using the total H2AX signal as reference) and normalized to the effect of 100 μM VP16 (set to 100%). Effects on HT-1080 and MRC-5 cells are represented by closed and open symbols, respectively. Insert: Rescaled representation of the genistein data. Where error bars are not shown, they are smaller than the symbols. (D) Quantitative comparison of Topo II–DNA linkage at various concentrations of VP16 or genistein (B) with corresponding γ-H2AX responses (according to the data set for HT-1080 cells in [C]). Dashed lines represent linear regression of the data. For genistein exposure of Topo IIα and IIβ, r^2–values were 0.91 and 0.95, respectively and the slopes were 0.029 and 0.03, respectively). For VP16 exposure of Topo IIα and IIβ, r^2-values were 0.93 and 0.97, respectively and the slopes were 0.28 and 0.29, respectively). (E) Representative images of HT-1080 cells expressing GFP-fused Topo IIα or IIβ scanned at 650-fold magnification in mid-plane before and after treatment with 50 μM VP16 (top) or 200 μM genistein (bottom). Each row of images shows from left to right the same cell nucleus before (phase contrast and green fluorescence) and 10 min after drug exposure (green fluorescence only). The μ-bar in the lower right corner applies to all images.

<0.001) were obtained assuming the coexistence of slow and fast enzyme populations with FRAP rate constants similar to those in untreated cells. However, in the presence of VP16, the two populations did not add up to 100% (as opposed to untreated cells, compare Fig. 1D), suggesting that VP16 induced an additional enzyme fraction imposing as ''immobile'' because it did not significantly contribute to fluorescence recovery during the 90 s observation window. ''Immobile'' fractions increased at the expense of fast and slow fractions in a dose-related manner. For Topo IIα (Fig. 3B, left), this effect reached saturation at 100 μM VP16 and encompassed ''immobilization'' of the entire cellular enzyme complement, whereas for Topo IIβ (Fig. 3B, right) saturation was reached at 400 μM VP16 and the maximal effect did not involve more than ≈50% of the enzyme molecules, indicating a lesser sensitivity of the β-isoform for VP16. FRAP measurements with an extended observation time window (Fig. 3C) showed that Topo IIα and IIβ were not

truly immobilized by saturation concentrations of VP16, but retained residual recovery rates of 0.132 ± 0.031 and 0.324 ± 018/min, respectively. This observation suggests that the Topo II–DNA cleavage complex stabilized by VP16 is dynamic and undergoes continuous DNA association/dissociation albeit at a much reduced rate. Mean DNA residence times of the DNA cleavage complex estimated from extended FRAP measurements [29–31] were 5.4 and 2.1 min for Topo IIα and IIβ, respectively, which is ≈10-fold longer than DNA residence times of the DNA-engaged enzymes in the absence of drug (21.6 ± 4.9 and 22.4 ± 5.3 s for Topo IIα and IIβ, respectively), but much shorter than DNA residence times of bona fide immobile nuclear proteins such as core histones which are in the range of hours [27, 37]. Reversal of retardation upon washout of VP16 had a half-time of 32 and 15 min for Topo IIα and IIβ, respectively (Fig. 3D). A similar time course has been observed for the reversal of VP16-induced Topo II–DNA linkage in human CEM cells measured by the ICE bioassay [17]. The time frame of complete reversal was about ten times as long as the mean

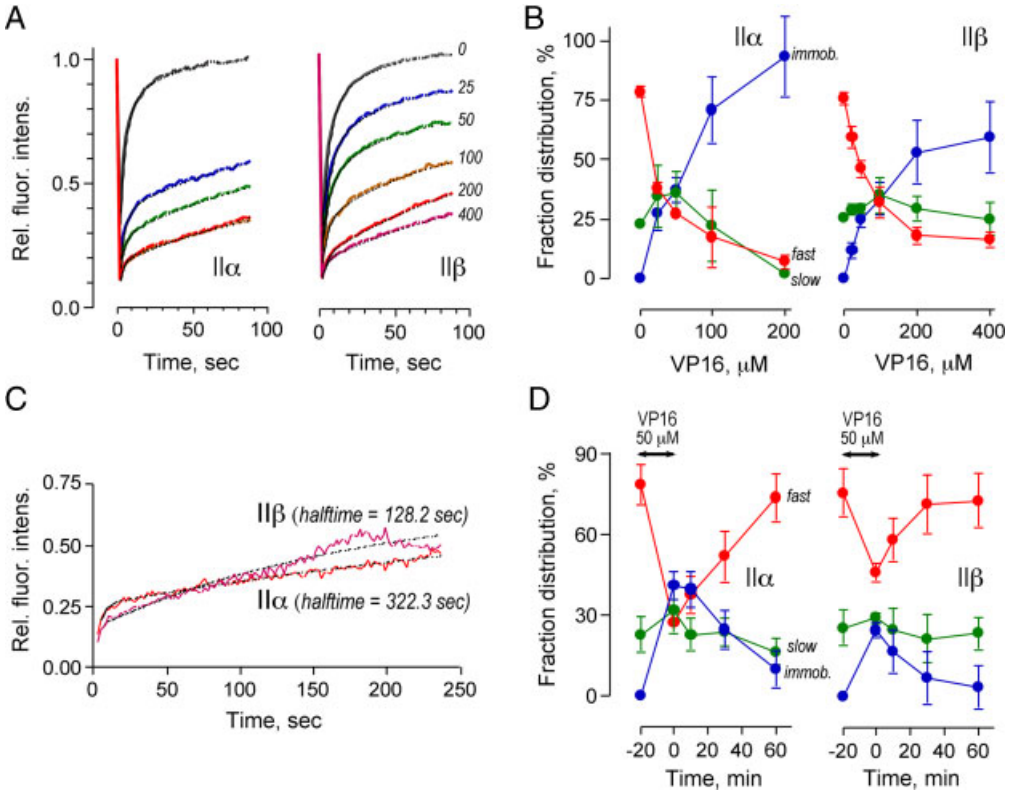

Figure 3. Impact of VP16 on ex vivo mobility of Topo IIα and IIβ. (A) Dose response: Nucleoplasmic FRAP recordings of Topo IIα-GFP (left) or IIβ-YFP (right) taken before (grey) or after exposure for 20 min to various concentrations [μM] of VP16 indicated on the right margin. Each curve represents the mean of eight independent FRAP recordings made in individual cells and normalized to a prebleach fluorescence level of 1. The standard error of the data was <5% (error bars omitted for clarity). Black dotted lines represent nonlinear regression of the data. Best fits were obtained with kinetic models, assuming that two enzyme fractions with fast and slow mobilities were present. (B) Relative amounts of fast (red) and slow enzyme fractions (green) and of a third, presumably immobile, fraction defined by the negative offset of maximal recovery from a value of 1 (blue) are plotted over concentration of VP16. Every data point represents the mean ± SEM of three independent experiments each consisting of eight individual FRAP recordings simultaneously subjected to regression analysis. Results for Topo IIα-GFP and IIβ-YFP are shown on the left and right hand side, respectively. (C) Determination of DNA residence times of Topo IIα (red) and Topo IIβ (magenta) in the presence of VP16 saturation (100 and 400 μM, respectively) by nucleoplasmic FRAP recordings with an extended observation window. The mean of five recordings in individual cells is shown. Dotted lines represent nonlinear regression of the data, assuming that three enzyme fractions with different mobilities are present. Derived recovery half-times of the slowest fractions are stated. (D) Reversal of VP16 effect: Nucleoplasmic FRAP recordings of Topo IIα-GFP (left) and IIβ-YFP (right) were taken before (−20 min) and after (0 min) equilibration with 50 μM VP16. The drug was then removed and further recordings were done at the indicated time points. Each data point represents the mean ± standard error of nonlinear regression analysis of three independent experiments each consisting of eight individual FRAP recordings simultaneously subjected to nonlinear regression analysis. In all cases, best fits were obtained with kinetic models, assuming that two enzyme fractions with fast and slow mobilities and a third, presumably immobile fraction defined by the offset of maximal recovery from a value of 1. Relative amounts of fast (red), slow (green), and immobile enzymes (blue) are plotted for Topo IIα-GFP (left) and -IIβ-YFP (right).

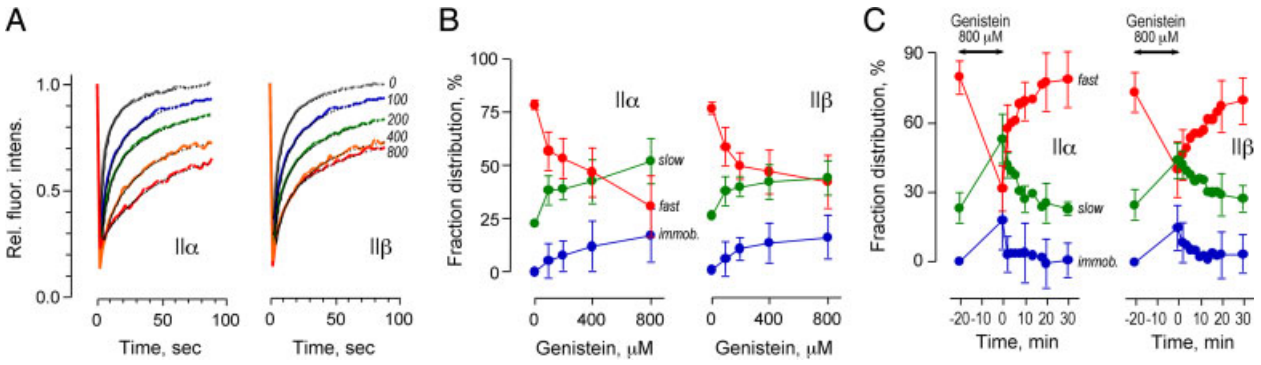

Figure 4. Impact of genistein on ex vivo mobility of Topo IIα and IIβ. Experimental conditions, replicates, and data processing are similar to corresponding sections of Fig. 3. (A) Dose response of nucleoplasmic FRAP of Topo IIα-GFP (left) or IIβ-YFP (right) to various concentrations [μM] of genistein indicated on the right margin. (B) Relative amounts of fast (red), slow (green), and presumably immobile enzyme fractions (blue) derived from nonlinear regression analysis are plotted against the concentration of genistein. (C) Reversal of genistein effect: Nucleoplasmic FRAP recordings of Topo IIα-GFP (left) or IIβ-GFP (right) were taken before (−20 min) equilibration with 800 μM genistein followed by drug removal (0 min) and further recordings at the indicated time points. FRAP data were subjected to nonlinear regression analysis and the resulting relative amounts of fast (red), slow (green), and immobile enzymes (blue) are plotted against time for Topo IIα-GFP (left) and IIβ-GFP (right).

DNA-residence time of the drug induced DNA–Topo II intermediate, suggesting that dissociation of the complex is indeed rate limiting for reversal.

A similar series of experiments carried out with genistein are shown in Fig. 4. Genistein also decreased mobility of Topo IIα and IIβ in a dose-dependent fashion. The effect was equilibrated within 20 min and effective concentrations ranged from 100 to 800 μM. Genistein effects on FRAP were similar for Topo IIα and IIβ, but much smaller than those of VP16. Moreover, the more rounded shape of the FRAP curves suggested a different mode of retardation (compare Figs. 3A and 4A). Nonlinear regression analysis confirmed this notion: Again, best fits of all FRAP curves were obtained assuming the coexistence of slow and fast enzyme fractions with rate constants similar to untreated cells. Retardation of Topo IIα and IIβ seemed mainly due to an increase in the slow (Fig. 4B, green symbols) at the expense of the fast (Fig. 4B, red symbols) enzyme fraction, whereas slower or immobile enzyme fractions were induced to a lesser degree (Fig. 4B, blue symbols, note data scatter relative to zero). In keeping with this, reversal of enzyme retardation at genistein saturation (800 μM) had a half-time of 1 and 3 min for Topo IIα and IIβ, respectively (Fig. 4C), which is in the range expected when reversal rates are determined by the normal DNA residence time of the isozymes deduced from the slow component of FRAP kinetics in untreated cells. In summary, these observations suggest that the primary effect of VP16 is recruitment of Topo IIα and IIβ to a DNA-bound form which has a ten-fold slower turnover and a ten-fold longer DNA residence time, whereas genistein enhances DNA recruitment of Topo IIα and IIβ without significantly prolonging DNA residence times of the enzymes or attenuating turnover of the enzyme–DNA complex. These findings are in good agreement with the notion that VP16 inhibits the religation step, whereas genistein stimulates the cleavage reaction of Topo II [39].

3.4 H2AX phosphorylation in response to VP16 or genistein corresponds to the extension of DNA residence time of Topo IIα and IIβ induced by the drugs

Figure 5A shows, at the top, a linear correlation between the disappearance of the fast moving fractions of Topo IIα and IIβ in response to increasing doses of VP16 or genistein (as determined by FRAP, see Figs. 3B and 4B) and a corresponding depletion of the specific protein bands of Topo IIα and IIβ from immunoblots (original blot data, see Supporting Information Fig. 2A). The stringency of the correlation strongly supports current belief that the fast fractions of Topo IIα and IIβ indeed represent enzyme molecules not engaged in DNA turnover [27, 28, 30, 37]. Therefore, they escape DNA linkage upon SDS denaturation and becoming detectable by immunoblotting. In keeping with this, covalent DNA–Topo II linkage measured by the ICE-bioassay exhibited a similarly stringent, albeit inverse correlation with the disappearance of the fast fractions of Topo IIα and IIβ in response to VP16 or genistein (Fig. 5A, bottom). Thus, drug-induced changes in the fast fractions of Topo II determined by FRAP can be taken as a robust reciprocal measure of enzyme–DNA linkage induced by Topo II poisoning. In the case of VP16, disappearance of the fast enzyme fractions was stringently correlated to an exponential rise in H2AX phosphorylation (Fig. 5B, left, circles and dotted lines), whereas such a correlation was clearly absent in the cellular response to genistein (Fig. 5B, left, squares). A similar discrepancy was observed when H2AX phosphorylation in response to VP16 or genistein

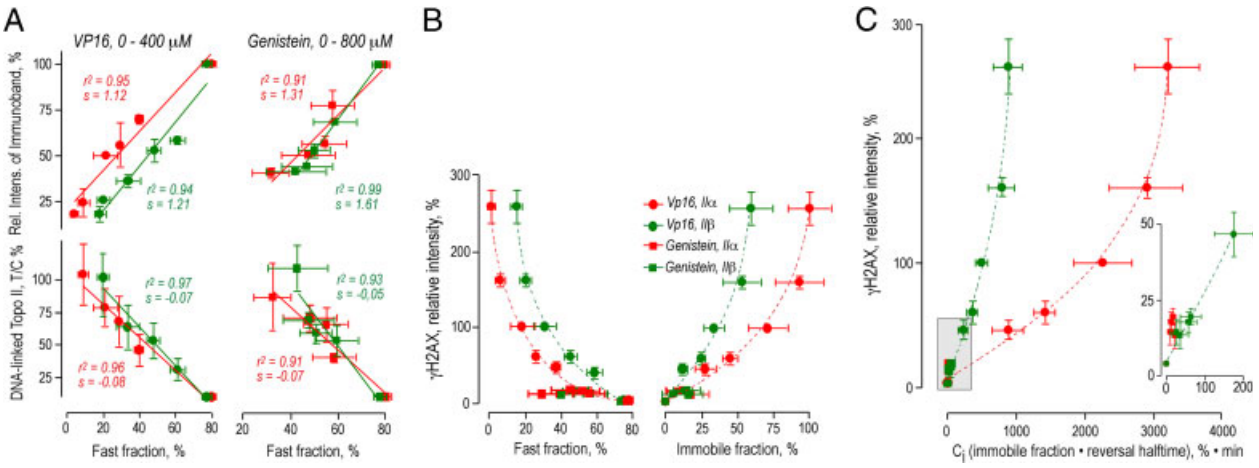

Figure 5. Comparison of H2AX phosphorylation, Topo II mobility, and Topo II–DNA linkage in response to VP16 and genistein. Data points represent the impact of VP16 (0, 25, 50, 100, 200, and 400 μM) (circles) or genistein (0, 100, 200, 400, and 800 μM) (squares) both on Topo IIα (red symbols), and Topo IIβ (green symbols). Mean values ± SEM of at least four independent determinations are shown. (A) Relative amounts of fast fraction derived from FRAP measurements (Figs. 3B and 4B) are plotted against relative intensity of residual specific protein band in immunoband depletion (top) or relative amount of enzyme linked to DNA (ICE bioassay) (bottom). The results of linear data regressions are represented by solid lines and both coefficients (r^2) and slopes (s) are stated next to the curves in matching colors. (B and C) γ-H2AX values (according to the data set for HT1080 cells in Fig. 2C) are plotted against relative amounts of fast (B, left) or immobile (B, right) fraction of Topo IIα or IIβ (derived from FRAP measurements, see Figs. 3B and 4B) or the coefficients of Topo II immobilization (C_i). Thus, the relative amounts of immobile fraction were multiplied by the half-times of reversal of immobilization after washout of the drugs (compare Figs. 3D and 4C), which in the case of VP16 were $t_{1/2} = 32 \pm 5$ and 15 ± 3 min for Topo IIα and IIβ, respectively, and in the case of genistein were $t_{1/2} = 1 \pm 0.5$ and 3 ± 0.8 min for Topo IIα and IIβ, respectively. Dotted lines in (B) and (C) represent nonlinear regression of the data using a model of single component exponential decay. R^2 was >0.97 throughout. (C) Significantly better correlations ($p < 0.001$, $\Delta R^2 > 0.05$) for Topo IIα, when data of genistein and VP16 were jointly subjected to regression. (D, inset): Enlarged representation of the portion shaded in grey in the main plot.

was compared with Topo II–DNA linkage measured by the ICE assay (Fig. 2D) or Topo II immunoband depletion (Supporting Information Fig. 2C). Thus, DNA entrapment and concomitant loss of free Topo II strongly reflected the genotoxicity of VP16 but not of genistein. Since genistein had a much lesser potency than VP16 to induce "immobile" Topo II (compare blue symbols in Figs. 3B and 4B), we speculated that it could be just the "immobile" portions of the enzymes that trigger H2AX phosphorylation. To check this, we plotted H2AX phosphorylation in response to various concentrations of VP16 or genistein against corresponding values of "immobile" fractions of Topo II (Fig. 5B, right). This improved coherence of the data sets for genistein and VP16, but did still not allow for joint regression of the data sets of the two drugs. To obtain this, we further had to factor in reversibility of drug-induced immobilization, which was much slower for VP16 ($t_{1/2} = 32 \pm 5$ and 15 ± 3 min for Topo IIα and IIβ, respectively) than for genistein ($t_{1/2} = 1 \pm 0.5$ and 3 ± 0.5 min for Topo IIα and IIβ, respectively Figs. 3D and 4C). When H2AX phosphorylation in response to various concentrations of VP16 or genistein was plotted against a compound value of the percentage of immobile fraction multiplied by the half-time of reversal (termed coefficient of immobilization, C_i; Fig. 5C), we obtained complete coherence of the data sets of VP16 and genistein for Topo IIβ. Significantly better correlations were obtained ($p < 0.001$, $\Delta r^2 > 0.05$) when these two data sets were combined in a single regression. The opposite was true for the Topo IIα data sets of VP16 and genistein, which exhibited better correlations when analyzed separately. An enlarged representation of the relevant portion of the plot (Fig. 5C, inset) shows that Topo IIβ data for genistein and VP16 (green squares and circles, respectively) aligned with high fidelity along a single exponential regression line (green dotted line). On the contrary, the Topo IIα data for genistein (red squares) were outliers to the left indicating a complete lack of correlation with H2AX phosphorylation. These observations suggest that the potency of VP16 and genistein to trigger Topo II-mediated DNA damage responses is covariant to their potency to recruit Topo II to a DNA bound form with a prolonged DNA residence time and to the reversal time of DNA residence time prolongation. In the case of genistein, this covariance existed only for the impact on the β isozyme. This finding would be meaningful if genistein exerts its (weak) DNA damaging effect solely through a moderate immobilization of the β-isoform, whereas its even lesser effect on the α-isoform is below the threshold of the cellular DNA damage response. In support of this, Topo II nucleolar depletion in response to genistein was found here restricted to the β-isoform (Fig. 2E).

3.5 Various types of Topo II poisons share a quantitative correlation between effects on DNA residence time and corresponding γH2AX responses

To test the general validity of our findings made with genistein and VP16, we carried out a survey on a range of Topo II poisons playing a class-representative role in tumor therapy or environment and food toxicology. Figure 6A shows that the DNA damaging potential of these substances varied over a wide range. Synthetic Topo II poisons with established anti-cancer activity (i.e. VP16, DOX, mAMSA, and MITOX) [6, 39] elicited higher DNA damage responses and/or were effective at lower concentrations than various plant polyphenols (genistein, EGCG) and natural food contaminants (AOH) [7, 15] or the benzoquinone metabolite NAPQI [11, 13]. The latter group exhibited a dose–response profile more similar to catalytic Topo II inhibitors of various chemical classes (ICRF-187, naphthoquinone, plumbagin) [40–42] than to classical Topo II poisons. To determine whether the lesser genotoxicity of these substances was due to a shorter half-life of the Topo II–DNA complexes induced, we determined the impact of their maximally DNA damaging dose on Topo II ex vivo mobility (defined by the fractions of Topo IIα and IIβ becoming immobile and the half-time of reversal of immobilization after washout of the drug). These results are summarized in Table 1. The various Topo II poisons used in cancer therapy exhibited a much higher potency to immobilize Topo IIα and IIβ than the various plant polyphenols or the toxic metabolite NAPQI, and this potency corresponded to their higher genotoxic potency (Fig. 6B, compare closed and open circles). Moreover, there was a stringent linear correlation ($r^2 = 0.89$) between these two potencies for all Topo II poisons tested (Fig. 6B, inset, closed circles). Thus, the DNA damaging potency of various chemically diverse Topo II poisons appears to be covariant with their potency to prolong DNA residence of Topo IIα and/or IIβ.

3.6 Catalytic Topo II inhibitors also share a quantitative correlation between prolongation of Topo II–DNA residence and γH2AX responses, albeit at a lower level of DNA damage

It stands to a reason that prolongation of Topo II–DNA residence by Topo II poisons reflects stabilization of the enzyme-coupled DNA double strand break, which is the common genotoxic mechanism of these compounds [6, 43]. However, this is just one of the several possible mechanisms by which Topo II–DNA residence could be prolonged and it cannot be excluded that immobilization of the enzymes per se also triggers damage recognition responses. To exclude this, we studied the effects of ICRF-187, which is a competitive inhibitor of Topo II ATPase activity required for reopening the enzyme clamp at the end of the catalytic cycle [40]. It thereby stabilizes a conformation of Topo II where the clamp of the enzyme remains closed around an unbroken DNA double strand [41]. Thus, ICRF-187 is expected to extend Topo II–DNA residence without inducing DNA cleavage. In our hands, this was indeed the case: ICRF-187 and several natural and synthetic naphthoquinones having a similar effect on Topo II activity [42] exhibited a potency to immobilize Topo IIα and IIβ that was similar or even higher than that of the most potent Topo II poisons (Table 1). However, corresponding γH2AX responses were much lower than for the Topo II poisons (Fig. 6B, compare squares and circles). In other words, γH2AX responses to immobilization of Topo II in the closed clamp formation on unbroken DNA are much lower than γH2AX responses to a quantitatively equal retardation of Topo II in the DNA-strand break coupled form. In keeping with current belief, this clearly indicates that prolongation of the covalently DNA-linked enzyme state is the major trigger for DNA damage responses. Yet it should be noted that within the group of catalytic Topo II inhibitors, there was also a stringent linear correlation between Topo II immobilization and (an overall much weaker) DNA damage response (Fig. 6B, inset, compare open and closed circles). This correlation may reflect the potency of these compounds to withdraw Topo II from essential cellular tasks, which is believed to be the common cytotoxic mechanism of catalytic Topo II inhibitors [6, 39].

4 Discussion

Our findings are relevant for the genotoxic risk assessment of micronutrients and environmental toxins that inflict Topo II-mediated DNA damage in humans. Most prominent among these are bioflavonoids, a diverse group of polyphenolic compounds found in fruits, vegetables, nuts, legumes, fungi, and plant leaves. Bioflavonoids are an integral component of human diets and the most abundant natural source of antioxidants [1, 3]. Epidemiological studies link the dietary intake of bioflavonoids to a lower incidence and/or prevalence of cancer, cardiovascular dysfunction, osteoporosis, inflammation, and other age-related diseases [5, 44–47]. Thus, increased consumption or diet fortification with bioflavonoids could be beneficial for human health. However, at increased concentrations, some bioflavonoids are likely to have serious adverse effects, inter alia because they poison human Topo I [48] and/or Topo II [7, 9, 15]. Topo poisoning is believed to contribute to the antitumor activity of some bioflavonoids [5, 6, 45] but can also compromise genome stability. Genistein has been demonstrated to induce DNA sequence rearrangements in mouse myeloid progenitor cells by a Topo IIβ and proteasome-mediated mechanism [49]. In human hematopoetic stem cells, genistein and two other widely consumed bioflavonoids (quercetin and kaempferol) trigger chromosomal rearrangements [50] believed to involve Topo II–DNA cleavage and known to cause childhood leukemia [51, 52]. In

Table 1. γH2AX response and corresponding impact on DNA residence of Topo IIα and IIβ

Compound	D_{max} (μM)[a]	γH2AX (%)[b]	Immobil. IIα(%)[c]	Immobil. IIα(min)[d]	C_i α(% min)[e]	Immobil. IIβ(%)[c]	Immobil. IIβ(min)[d]	C_i β(% min)[e]
VP16	200	164.3±10 (3)[f]	93±15 (8)	32±5 (5)	2976±75	59±15 (5)	15±3 (5)	885±45
mAMSA	10	81.4±5 (3)	37±5 (4)	8±2 (3)	296±10	22±2 (3)	11±3 (3)	242±6
DOX	3.125	21.3±11 (5)	16±4 (5)	45±15 (3)	720±35	32±7 (5)	23±4 (3)	736±28
MITOX	1	70±10 (4)	25±5 (3)	120 (3)	3000	28±5 (3)	120 (3)	3360
NAPHQI	100	4.7±3 (3)	8.5	1	8.5	3.9	1	3.9
Genistein	400	21.6±4 (3)	12±7 (5)	1± 0.5 (5)	12±3.5	15±10 (5)	3± 0.5 (5)	45±5
AOH	200	12±2 (3)	9±3 (3)	2±0,5 (3)	18±2	6±4 (3)	5±1 (3)	30±4
EGCG	100	6.2±0.9 (3)	6.5	2	13	2.9	1	2.9
Quercetin	200	4.1±1.2 (3)	0 (3)	ND[g]	ND	0 (3)	ND	ND
Epicatechin	200	3.9	0	ND	ND	0	ND	ND
ICRF187	200	19±15 (3)	58±16	120	6960	65±18	180	11700
Naphthoquinone[h]	100	19	79±10 (3)	120	9480	84±4 (3)	120	10080
Plumbagin	50	14±5 (2)	28±8 (3)	40	1120	28±9 (3)	40	1120
Menadione	50	3.7	0 (3)	ND	ND	0 (3)	ND	ND
Lawsone	50	3.9	0 (3)	ND	ND	0 (3)	ND	ND
Juglone	50	3.8	0 (3)	ND	ND	0 (3)	ND	ND
solvent control		4±0.4 (6)	ND	ND	ND	ND	ND	ND

a) Dose of maximal H2AX phosphorylation, derived from dose–response analysis shown in Fig. 6A.
b) Maximal γH2AX response determined by immunoblotting and densitometry (see Fig. 2 C); data are normalized to the effect of 100 μM VP16 (= 100%).
c) Fraction of enzyme that at dose of maximal γH2AX response appears immobile or has a >10-fold lower FRAP rate than in the absence of drug.
d) Half-time of disappearance of immobile enzyme fraction after the removal of drug (see Fig. 3D).
e) Coefficient of immobility at dose of maximal γH2AX response (= immobile enzyme fraction multiplied with half-time of reversal after drug removal).
f) Whenever applicable, mean±SEM is given and the number of independent determinations is stated in parenthesis.
g) Determination not meaningful.
h) Forward rate of FRAP recovery of immobile state measured as 10−5/min for both isoforms.

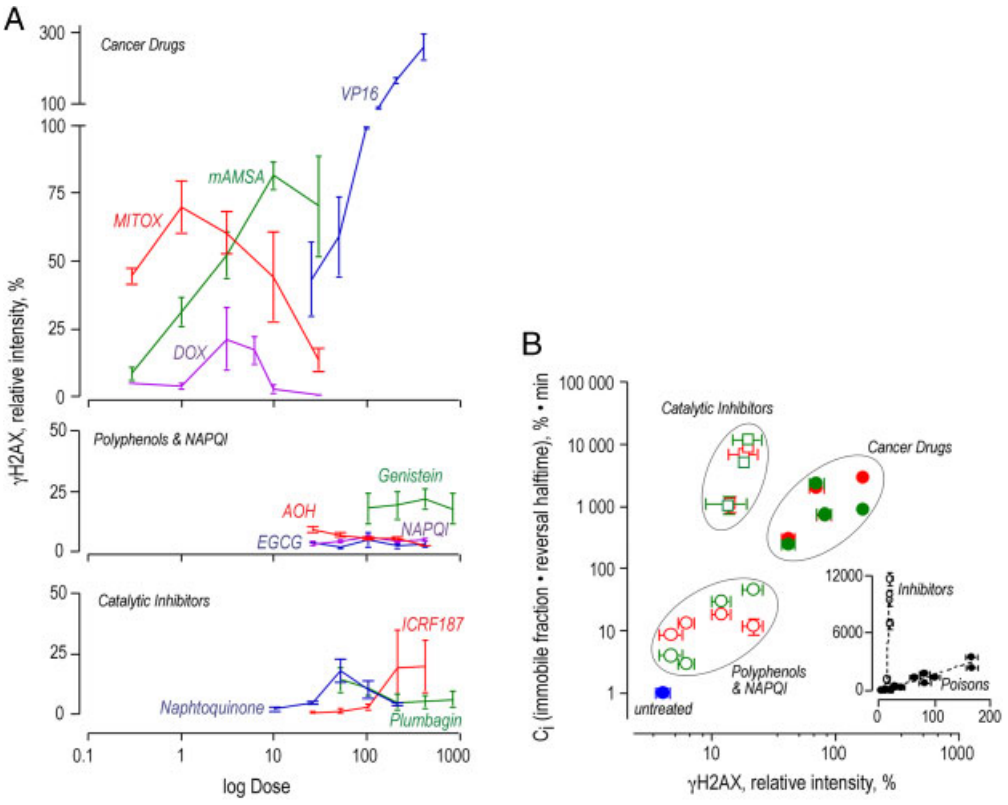

Figure 6. Comparison of Topo II immobilization and γH2AX response to various Topo II poisons and catalytic inhibitors. Mean values ± SEM of at least three independent determinations are shown. (A) HT-1080 cells were incubated (1 h, 37°C) with various concentrations of the drugs and H2AX phosphorylation was assessed by comparative immunoblotting with a monoclonal antibody against γ-H2AX (phosphorylated at Ser 139). Data are corrected for loading and normalized to the effect of 100 μM VP16 (set to 100%). Top, middle, and bottom panel are set to identical scale. (B) Results of graphic analysis are summarized in Table 1: C_i-values of Topo II immobilization (calculated as in Fig. 5C) determined at strongest/highest DNA-damaging concentrations of various Topo II-targeted compounds (derived from [A]) are plotted against corresponding γ-H2AX responses. Data for Topo IIα and IIβ are indicated by red and green symbols, respectively. Closed circles represent Topo II poisons with established anticancer activity (VP16, MITOX, DOX, mAMSA, and XK469). Open circles represent natural polyphenols (genistein, EGCG, and AOH) or toxic drug metabolites (NAPQI) known to induce Topo II-mediated DNA cleavage. Open squares represent synthetic and natural compounds known to act as catalytic inhibitors by stabilizing the closed clamp formation of Topo II (ICRF-187, naphthoquinone, and plumbagine). Blue square: Cell background treated with solvent control. (B, inset) Linear regression of entire data sets for Topo II poisons (closed circles) or catalytic inhibitors (open circles) with r^2-values of 0.89 and 0.91, respectively and the slopes of 0.0006 and 0.073, respectively.

keeping with this, enhanced maternal consumption of genistein has been associated with a ten-fold increased risk of infant acute myelogenous leukemia [53]. In summary, increased uptake of bioflavonoids and other natural and environmental compounds that poison Topo II appears to bear a significant genotoxic risk advocating a systematic quantitative assessment of this potency.

Currently, natural or environmental Topo II poisons are recognized by their potency to induce Topo II-mediated DNA cleavage or Topo II–DNA linkage [9, 11–13, 54]. However, it has been recently shown that the DNA-damaging potential of two compounds with an comparable Topo II poisoning potency (genistein and VP16) is not reflected by the levels of Topo II–DNA cleavage complexes induced but by the persistence of such complexes in the cell [17]. We show here that this difference is faithfully reflected by corresponding prolongation of Topo II–DNA residence in the living cell. We find that attenuation of Topo II interaction kinetics is covariant with cellular DNA damage response over the entire dose–response ranges of genistein and VP16, and we find the same quantitative correlation in several other archetypical Topo II poisons of various chemical classes. Using catalytic Topo II inhibitors, we exclude that attenuation of Topo II interaction kinetics per se elicits DNA damage responses at a similar level. We conclude from these findings that there exists a relationship between DNA damage response and the persistence of Topo II–DNA cleavage complexes that is the same for many (if not all) Topo II poisons. Thus, the contribution of Topo II poisoning to the genotoxic potential of a given compound could possibly be gauged more appropriately by measuring persistence of Topo II–DNA cleavage complexes in addition

to the extent of Topo II–DNA cleavage. Alterations of Topo II DNA interaction kinetics seem to be a valid measure for the persistence of drug-induced Topo II–DNA cleavage complexes in the cell since they not only reflect the known properties of genistein and VP16 in this respect [17] but also conform to the published knowledge on the cellular persistence of Topo II–DNA cleavage complexes induced by various other therapeutic Topo II poisons [55].

As compared with therapeutic Topo II poisons, dietary Topo II poisons tested in this study had only moderate or no effects on Topo II–DNA residence, irrespective of whether they inhibit Topo II DNA religation (e.g. NAPQI) [11] or stimulate Topo II DNA cleavage by enzyme binding (e.g. quercetin) or redox cycling (e.g. EGCG) [7]. In all these cases, moderate or absent effects on Topo II–DNA interaction kinetics were matched by low or absent DNA damage responses. In principle, this could be due to simultaneous triggering of other pathways such as tyrosine kinase inhibition or displacement of Topo II from DNA. However, it has been previously demonstrated that the lower genotoxicity of genistein in comparison to VP16 does not result from non-Topo II-directed activities [17]. We show that none of the tested isoflavones and other dietary Topo II poisons clusters in the correlative matrix together with catalytic inhibitors of Topo II ATPase such as ICRF 187 or plumbagin. This virtually excludes that these compounds inhibit Topo II ATPase activity and thereby attenuate their Topo II poisoning effects. Another possible interference could be with γH2AX as a readout of DNA damage. Histone 2AX is phosphorylated by members of the phosphatidylinositol 3-kinase-like kinase (PIKK) family, including ATM, ATR, and DNA-PK [56, 57], which can be influenced by protein kinase inhibitors [25, 57]. Therefore, tyrosine kinase inhibitory properties of the tested compounds could, in principle, lead to the suppression of phosphorylation of histone 2AX. This would be most probable in the case of genistein which is a known tyrosin kinase inhibitor [58]. However, genistein is unlikely to inhibit those phosphatidylinositol 3-kinase-like kinase family members that are responsible for histone 2AX phosphorylation, because it has been demonstrated that genistein induces phosphorylation of ATM and histone 2AX and that ATM phosphorylates H2AX in response to genistein-induced DNA double-strand breakage [59]. Thus, the lesser impact of genistein on Topo II–DNA residence (as compared with therapeutic Topo II poisons) is most probably due to the fact that the Topo II–DNA intermediates thereby induced are too short-lived to elicit significant DNA damage responses. It seems likely that this also holds true for the other isoflavones and dietary Topo II poisons tested here, which exhibited the effects on Topo II–DNA residence that were even more transient than the ones of genistein.

Interestingly, genistein had a comparable impact on DNA cleavage of both Topo II isoforms. However, its (moderate) impact on DNA residence was significant only for Topo IIβ and only these data points fitted the correlative matrix with H2AX phosphorylation. This seems to indicate that genistein, although poisoning both isoforms to a similar extent, exerts its DNA-damaging effect mostly through its more stable interaction with Topo IIβ. This notion is corroborated by the observations that cells lacking Topo IIβ are resistant to genistein [60]. Given that regulation of transcription by various steroids involves stimulation of Topo IIβ-mediated DNA cleavage [61, 62], the known estrogen-like properties of genistein [1, 63, 64] could selectively boost its impact on Topo IIβ–DNA interaction in cells expressing estrogen receptors. However, a similar effect was also found with the mycotoxin AOH not rated a phytoestrogen, whereas it was not found with quercetin which, like genistein, acts as phytoestrogen and Topo II poison. Thus, it remains unclear how the Topo II isoform is selected that mediates the genotoxic effect of a given isoflavone or other dietary Topo II poison. However, this selection is important, because current belief holds that poisoning of Topo IIα mediates tumor cell killing, whereas poisoning of Topo IIβ promotes mutagenesis and cancerogenesis [65]. Along these lines, Topo IIβ-mediated DNA damage by genistein fits the mutagenic potential of this isoflavone that has been established at the level of the cell [49] and the human population [53].

This finally raises the question of how relevant are the genotoxic effects of genistein demonstrated here in the light of what is known about the intake and bioavailability of dietary isoflavones in humans? The average dietary intake of soy-derived isoflavones is less than 1 mg/day in western countries, whereas in Asia it amounts up to 50 mg/day [2, 66]. This results in plasma concentrations in the lower nanomolar range for western countries and around 870 nM for Asian countries [3, 67]. Bioavailability of genistein appears to be not significantly different when isoflavones are consumed as aglycones or glucosides [68] because the glucosides are substrates for bacterial β-glucosidases that release the aglycone forms in the jejunum [69]. The aglycones are either absorbed intact or further metabolized by intestinal microflora before absorption. Therefore, bioavailability is increased by a rapid gut transit time and low fecal digestion rates and decreased by a fiber-rich diet [2]. Aglycones of isoflavones seem to be transported much more efficiently than their respective glycosides [70] and are able to penetrate cells in contrast to the glycosides. However, there are no studies available stating actual isoflavone levels found in human cells in vivo. It seems unlikely that intracellular levels are much higher than those in human plasma, which rarely exceed 1 μM under normal nutrition [3] and may assume ten-fold this value under habitual consumption of dietary supplements based on soy extracts or of food products fortified with isoflavones in a purified form, which can raise daily isoflavone uptake up to 150 mg [66]. When comparing these approximative values of bioavailability with ex vivo dose responses of Topo IIβ-mediated DNA damage to the intact aglycon of genistein shown in this study, it seems unlikely that genistein has genotoxic or mutagenic effects when consumed in the course of normal

nutrition, whereas habitual consumption of dietary supplements based on soy extracts or of food products fortified with isoflavones could indeed contribute to the increase in mutagenic risk suggested by epidemiological studies[53].

This work was supported by the Deutsche Forschungsgemeinschaft, grant SFB 728, A1.

The authors have declared no conflict of interest.

5 References

[1] Ross, J. A., Kasum, C. M., Dietary flavonoids: bioavailability, metabolic effects, and safety. *Ann. Rev. Nutr.* 2002, *22*, 19–34.

[2] Nielsen, I. L., Williamson, G., Review of the factors affecting bioavailability of soy isoflavones in humans. *Nutr. Cancer* 2007, *57*, 1–10.

[3] Scalbert, A., Williamson, G., Dietary intake and bioavailability of polyphenols. *J. Nutr.* 2000, *130*, 2073S–2085S.

[4] Shimizu, H., Ross, R. K., Bernstein, L., Yatani, R. et al., Cancers of the prostate and breast among Japanese and white immigrants in Los Angeles County. *Br. J. Cancer* 1991, *63*, 963–966.

[5] Kandaswami, C., Lee, L. T., Lee, P. P., Hwang, J. J. et al., The antitumor activities of flavonoids. *In vivo* 2005, *19*, 895–909.

[6] Nitiss, J. L., Targeting DNA topoisomerase II in cancer chemotherapy. *Nat. Rev.* 2009, *9*, 338–350.

[7] Bandele, O. J., Clawson, S. J., Osheroff, N., Dietary polyphenols as topoisomerase II poisons: B ring and C ring substituents determine the mechanism of enzyme-mediated DNA cleavage enhancement. *Chem. Res. Toxicol.* 2008, *21*, 1253–1260.

[8] Barthelmes, H. U., Niederberger, E., Roth, T., Schulte, K. et al., Lycobetaine acts as a selective topoisomerase II beta poison and inhibits the growth of human tumour cells. *Br. J. Cancer* 2001, *85*, 1585–1591.

[9] Fehr, M., Pahlke, G., Fritz, J., Christensen, M. O. et al., Alternariol acts as a topoisomerase poison, preferentially affecting the IIalpha isoform. *Mol. Nutr. Food Res.* 2009, *53*, 441–451.

[10] Habermeyer, M., Fritz, J., Barthelmes, H. U., Christensen, M. O. et al., Anthocyanidins modulate the activity of human DNA topoisomerases I and II and affect cellular DNA integrity. *Chem. Res. Toxicol.* 2005, *18*, 1395–1404.

[11] Bender, R. P., Lindsey, R. H., Jr., Burden, D. A., Osheroff, N., N-acetyl-p-benzoquinone imine, the toxic metabolite of acetaminophen, is a topoisomerase II poison. *Biochemistry* 2004, *43*, 3731–3739.

[12] Lindsey, R. H., Jr., Bender, R. P., Osheroff, N., Effects of benzene metabolites on DNA cleavage mediated by human topoisomerase II alpha: 1,4-hydroquinone is a topoisomerase II poison. *Chem. Res. Toxicol.* 2005, *18*, 761–770.

[13] Lindsey, R. H., Bender, R. P., Osheroff, N., Stimulation of topoisomerase II-mediated DNA cleavage by benzene metabolites. *Chem. Biol. Interact.* 2005, *153–154*, 197–205.

[14] Willmore, E., Frank, A. J., Padget, K., Tilby, M. J., Austin, C. A., Etoposide targets topoisomerase IIalpha and IIbeta in leukemic cells: isoform-specific cleavable complexes visualized and quantified in situ by a novel immunofluorescence technique. *Mol. Pharmacol.* 1998, *54*, 78–85.

[15] Bandele, O. J., Osheroff, N., Bioflavonoids as poisons of human topoisomerase II alpha and II beta. *Biochemistry* 2007, *46*, 6097–6108.

[16] Muslimovic, A., Nystrom, S., Gao, Y., Hammarsten, O., Numerical analysis of etoposide induced DNA breaks. *PloS One* 2009, *4*, e5859.

[17] Bandele, O. J., Osheroff, N., The efficacy of topoisomerase II-targeted anticancer agents reflects the persistence of drug-induced cleavage complexes in cells. *Biochemistry* 2008, *47*, 11900–11908.

[18] Soubeyrand, S., Pope, L., Hache, R. J., Topoisomerase IIalpha-dependent induction of a persistent DNA damage response in response to transient etoposide exposure. *Mol. Oncol.* 2010, *4*, 38–51.

[19] Furuta, T., Takemura, H., Liao, Z. Y., Aune, G. J. et al., Phosphorylation of histone H2AX and activation of Mre11, Rad50, and Nbs1 in response to replication-dependent DNA double-strand breaks induced by mammalian DNA topoisomerase I cleavage complexes. *J. Biol. Chem.* 2003, *278*, 20303–20312.

[20] Banath, J. P., Olive, P. L., Expression of phosphorylated histone H2AX as a surrogate of cell killing by drugs that create DNA double-strand breaks. *Cancer Res.* 2003, *63*, 4347–4350.

[21] MacPhail, S. H., Banath, J. P., Yu, T. Y., Chu, E. H. et al., Expression of phosphorylated histone H2AX in cultured cell lines following exposure to X-rays. *Int. J. Radiat. Biol.* 2003, *79*, 351–358.

[22] MacPhail, S. H., Banath, J. P., Yu, Y., Chu, E., Olive, P. L., Cell cycle-dependent expression of phosphorylated histone H2AX: reduced expression in unirradiated but not X-irradiated G1-phase cells. *Radiat. Res.* 2003, *159*, 759–767.

[23] Bonner, W. M., Redon, C. E., Dickey, J. S., Nakamura, A. J. et al., GammaH2AX and cancer. *Nat. Rev.* 2008, *8*, 957–967.

[24] Dickey, J. S., Redon, C. E., Nakamura, A. J., Baird, B. J. et al., H2AX: functional roles and potential applications. *Chromosoma* 2009, *118*, 683–692.

[25] Watters, G. P., Smart, D. J., Harvey, J. S., Austin, C. A., H2AX phosphorylation as a genotoxicity endpoint. *Mutat. Res.* 2009, *679*, 50–58.

[26] Mah, L. J., El-Osta, A., Karagiannis, T. C., gammaH2AX: a sensitive molecular marker of DNA damage and repair. *Leukemia* 2010, *24*, 679–686.

[27] Christensen, M. O., Larsen, M. K., Barthelmes, H. U., Hock, R. et al., Dynamics of human DNA topoisomerases IIalpha and IIbeta in living cells. *J. Cell Biol.* 2002, *157*, 31–44.

[28] Phair, R. D., Misteli, T., High mobility of proteins in the mammalian cell nucleus. *Nature* 2000, *404*, 604–609.

[29] Athale, C. A., Christensen, M. O., Eils, R., Boege, F., Mielke, C., Inferring a system model of subcellular topoisomerase II beta localization dynamics. *Omics* 2004, *8*, 167–175.

[30] Schmiedeberg, L., Weisshart, K., Diekmann, S., Meyer Zu Hoerste, G., Hemmerich, P., High- and low-mobility populations of HP1 in heterochromatin of mammalian cells. *Mol. Biol. Cell* 2004, *15*, 2819–2833.

[31] Christensen, M. O., Barthelmes, H. U., Feineis, S., Knudsen, B. R. et al., Changes in mobility account for camptothecin-induced subnuclear relocation of topoisomerase I. *J. Biol. Chem.* 2002, *277*, 15661–15665.

[32] Linka, R. M., Porter, A. C., Volkov, A., Mielke, C. et al., C-terminal regions of topoisomerase IIalpha and IIbeta determine isoform-specific functioning of the enzymes in vivo. *Nucl. Acids Res.* 2007, *35*, 3810–3822.

[33] Boege, F., Andersen, A., Jensen, S., Zeidler, R., Kreipe, H., Proliferation-associated nuclear antigen Ki-S1 is identical with topoisomerase II alpha. Delineation of a carboxy-terminal epitope with peptide antibodies. *Am. J. Pathol.* 1995, *146*, 1302–1308.

[34] Subramanian, D., Furbee, C. S., Muller, M. T., ICE bioassay. Isolating in vivo complexes of enzyme to DNA. *Methods Mol. Biol.* 2001, *95*, 137–147.

[35] Kern, M., Fridrich, D., Reichert, J., Skrbek, S. et al., Limited stability in cell culture medium and hydrogen peroxide formation affect the growth inhibitory properties of delphinidin and its degradation product gallic acid. *Mol. Nutr. Food Res.* 2007, *51*, 1163–1172.

[36] Meyer, K. N., Kjeldsen, E., Straub, T., Knudsen, B. R. et al., Cell cycle-coupled relocation of types I and II topoisomerases and modulation of catalytic enzyme activities. *J. Cell Biol.* 1997, *136*, 775–788.

[37] Misteli, T., Gunjan, A., Hock, R., Bustin, M., Brown, D. T., Dynamic binding of histone H1 to chromatin in living cells. *Nature* 2000, *408*, 877–881.

[38] Baldwin, E. L., Osheroff, N., Etoposide, topoisomerase II and cancer. *Curr. Med. Chem.* 2005, *5*, 363–372.

[39] Pommier, Y., Leo, E., Zhang, H. L., Marchand, C., DNA topoisomerases and their poisoning by anticancer and antibacterial drugs. *Chem. Biol.* 2010, *17*, 421–433.

[40] Classen, S., Olland, S., Berger, J. M., Structure of the topoisomerase II ATPase region and its mechanism of inhibition by the chemotherapeutic agent ICRF-187. *Proc. Natl. Acad. Sci. USA* 2003, *100*, 10629–10634.

[41] Roca, J., Ishida, R., Berger, J. M., Andoh, T., Wang, J. C., Antitumor bisdioxopiperazines inhibit yeast DNA topoisomerase II by trapping the enzyme in the form of a closed protein clamp. *Proc. Natl. Acad. Sci. USA* 1994, *91*, 1781–1785.

[42] Jimenez-Alonso, S., Orellana, H. C., Estevez-Braun, A., Ravelo, A. G. et al., Design and synthesis of a novel series of pyranonaphthoquinones as topoisomerase II catalytic inhibitors. *J. Med. Chem.* 2008, *51*, 6761–6772.

[43] Liu, L. F., DNA topoisomerase poisons as antitumor drugs. *Annu. Rev. Biochem.* 1989, *58*, 351–375.

[44] Sies, H., Schewe, T., Heiss, C., Kelm, M., Cocoa polyphenols and inflammatory mediators. *Am. J. Clin. Nutr.* 2005, *81*, 304S–312S.

[45] Siddiqui, I. A., Adhami, V. M., Saleem, M., Mukhtar, H., Beneficial effects of tea and its polyphenols against prostate cancer. *Mol. Nutr. Food Res.* 2006, *50*, 130–143.

[46] Usui, T., Pharmaceutical prospects of phytoestrogens. *Endocr. J.* 2006, *53*, 7–20.

[47] Schroeter, H., Heiss, C., Balzer, J., Kleinbongard, P. et al., (-)-Epicatechin mediates beneficial effects of flavanol-rich cocoa on vascular function in humans. *Proc. Natl. Acad. Sci. USA* 2006, *103*, 1024–1029.

[48] Boege, F., Straub, T., Kehr, A., Boesenberg, C. et al., Selected novel flavones inhibit the DNA binding or the DNA religation step of eukaryotic topoisomerase I. *J. Biol. Chem.* 1996, *271*, 2262–2270.

[49] Azarova, A. M., Lin, R. K., Tsai, Y. C., Liu, L. F. et al., Genistein induces topoisomerase IIbeta- and proteasome-mediated DNA sequence rearrangements: Implications in infant leukemia. *Biochem. Biophys. Res. Commun.* 2010, *399*, 66–71.

[50] Barjesteh van Waalwijk van Doorn-Khosrovani, S., Janssen, J., Maas, L. M., Godschalk, R. W. et al., Dietary flavonoids induce MLL translocations in primary human CD34+cells. *Carcinogenesis* 2007, *28*, 1703–1709.

[51] Strick, R., Strissel, P. L., Borgers, S., Smith, S. L., Rowley, J. D., Dietary bioflavonoids induce cleavage in the MLL gene and may contribute to infant leukemia. *Proc. Natl. Acad. Sci. USA* 2000, *97*, 4790–4795.

[52] Felix, C. A., Kolaris, C. P., Osheroff, N., Topoisomerase II and the etiology of chromosomal translocations. *DNA Repair* 2006, *5*, 1093–1108.

[53] Ross, J. A., Dietary flavonoids and the MLL gene: a pathway to infant leukemia? *Proc. Natl. Acad. Sci. USA* 2000, *97*, 4411–4413.

[54] Gao, H., Huang, K.-C., Yamasaki, E., Chan, K. et al., XK469, a selective topoisomerase IIβ poison. *Proc. Natl. Acad. Sci. USA* 1999, *96*, 12168–12173.

[55] Errington, F., Willmore, E., Leontiou, C., Tilby, M. J., Austin, C. A., Differences in the longevity of topo IIalpha and topo IIbeta drug-stabilized cleavable complexes and the relationship to drug sensitivity. *Cancer Chemother. Pharmacol.* 2004, *53*, 155–162.

[56] Burma, S., Chen, B. P., Murphy, M., Kurimasa, A., Chen, D. J., ATM phosphorylates histone H2AX in response to DNA double-strand breaks. *J. Biol. Chem.* 2001, *276*, 42462–42467.

[57] Stiff, T., O'Driscoll, M., Rief, N., Iwabuchi, K. et al., ATM and DNA-PK function redundantly to phosphorylate H2AX after exposure to ionizing radiation. *Cancer Res.* 2004, *64*, 2390–2396.

[58] Akiyama, T., Ishida, J., Nakagawa, S., Ogawara, H. et al., Genistein, a specific inhibitor of tyrosine-specific protein kinases. *J. Biol. Chem.* 1987, *262*, 5592–5595.

[59] Ye, R., Goodarzi, A. A., Kurz, E. U., Saito, S. et al., The isoflavonoids genistein and quercetin activate different stress signaling pathways as shown by analysis of site-

specific phosphorylation of ATM, p53 and histone H2AX. *DNA Repair* 2004, *3*, 235–244.

[60] Lopez-Lazaro, M., Willmore, E., Austin, C. A., Cells lacking DNA topoisomerase II beta are resistant to genistein. *J. Nat. Prod.* 2007, *70*, 763–767.

[61] Haffner, M. C., Aryee, M. J., Toubaji, A., Esopi, D. M. et al., Androgen-induced TOP2B-mediated double-strand breaks and prostate cancer gene rearrangements. *Nat. Genet.* 2010, *42*, 668–675.

[62] Ju, B. G., Lunyak, V. V., Perissi, V., Garcia-Bassets, I. et al., A topoisomerase IIbeta-mediated dsDNA break required for regulated transcription. *Science* 2006, *312*, 1798–1802.

[63] Doerge, D. R., Sheehan, D. M., Goitrogenic and estrogenic activity of soy isoflavones. *Environ. Health Perspect.* 2002, *110*, 349–353.

[64] Dixon, R. A., Phytoestrogens. *Ann. Rev. Plant Biol.* 2004, *55*, 225–261.

[65] Azarova, A. M., Lyu, Y. L., Lin, C. P., Tsai, Y. C. et al., Roles of DNA topoisomerase II isozymes in chemotherapy and secondary malignancies. *Proc. Natl. Acad. Sci. USA* 2007, *104*, 11014–11019.

[66] Mortensen, A., Kulling, S. E., Schwartz, H., Rowland, I. et al., Analytical and compositional aspects of isoflavones in food and their biological effects. *Mol. Nutr. Food Res.* 2009, *53*, S266–S309.

[67] Adlercreutz, H., Markkanen, H., Watanabe, S., Plasma concentrations of phyto-oestrogens in Japanese men. *Lancet* 1993, *342*, 1209–1210.

[68] Zubik, L., Meydani, M., Bioavailability of soybean isoflavones from aglycone and glucoside forms in American women. *Am. J. Clin. Nutr.* 2003, *77*, 1459–1465.

[69] Day, A. J., DuPont, M. S., Ridley, S., Rhodes, M. et al., Deglycosylation of flavonoid and isoflavonoid glycosides by human small intestine and liver beta-glucosidase activity. *FEBS Lett.* 1998, *436*, 71–75.

[70] Andlauer, W., Kolb, J., Stehle, P., Furst, P., Absorption and metabolism of genistein in isolated rat small intestine. *J. Nutr.* 2000, *130*, 843–846.

